Crosslinking a lipid raft component triggers liquid ordered–liquid disordered phase separation in model plasma membranes

A. T. Hammond*, F. A. Heberle†, T. Baumgart‡, D. Holowka*, B. Baird*, and G. W. Feigenson†§

Departments of *Chemistry and Chemical Biology, †Molecular Biology and Genetics, and ‡Applied and Engineering Physics, Cornell University, Ithaca, NY 14853

Edited by Kai Simons, Max Planck Institute of Molecular Cell Biology and Genetics, Dresden, Germany, and approved March 26, 2005 (received for review August 3, 2004)

The mechanisms by which a cell uses and adapts its functional membrane organization are poorly understood and are the subject of ongoing investigation and discussion. Here, we study one proposed mechanism: the crosslinking of membrane components. In immune cell signaling (and other membrane-associated processes), a small change in the clustering of specific membrane proteins can lead to large-scale reorganizations that involve numerous other membrane components. We have investigated the large-scale physical effect of crosslinking a minor membrane component, the ganglioside GM_1, in simple lipid models of the plasma membrane containing sphingomyelin, cholesterol, and phosphatidylcholine. We observe that crosslinking GM_1 can cause uniform membranes to phase-separate into large, coexistent liquid ordered and liquid disordered membrane domains. We also find that this lipid separation causes a dramatic redistribution of a transmembrane peptide, consistent with a raft model of membrane organization. These experiments demonstrate a mechanism that could contribute to the effects of crosslinking observed in cellular processes: Domains induced by clustering a small number of proteins or lipids might rapidly reorganize many other membrane proteins.

ganglioside | clustering | cholera toxin | bilayer

Crosslinking or clustering of specific biological membrane components is an indispensable element of many membrane-associated processes. In receptor signaling, transport vesicle biogenesis, cell polarization, and viral budding, a critical clustering event coincides with and is necessary for the initiation of a complex cellular process. Proposed mechanisms for these observations vary significantly between different experimental systems, and there is no expectation that the same mechanism should apply to each case. However, a recurring theme is that crosslinking (clustering or oligomerization) induces or stabilizes a structure that then recruits downstream machinery (1–6). The correlation between crosslinking and membrane domain formation is particularly well established for immune-recognition receptor signaling in B, T, and mast cells (7–10). Here, we demonstrate in simple model membranes that crosslinking of a minor lipid species can induce membrane domains to form by promoting large-scale phase separation.

The lipid raft hypothesis (1, 11) is a prominent model of cellular membrane organization. Discussions of individual cellular membrane functions often invoke the involvement of lipid rafts. This model proposes that some membrane proteins are segregated from each other by their preferential partitioning into regions of different membrane order, perhaps different phase, within a continuous cellular membrane. The interplay between lipid membrane phase behavior and lateral protein distribution is proposed to be involved in fundamental membrane-associated cellular processes, including signaling, endocytosis, exocytosis, protein sorting, polarization, motility, and several stages in the infectious cycle of many viruses (1–4, 6, 11–16).

Membrane phase behavior has been studied in mixtures of membrane-forming lipids for many decades (17, 18), and these early studies were important in developing the fluid mosaic model of cellular membranes (19). Subsequent studies of biological membrane heterogeneity and the role of cholesterol have refined this view and now define two different fluid phases: liquid disordered (Ld, also called Lα) and liquid ordered (Lo) (1, 20). The raft hypothesis proposes that some of the observed heterogeneity of biological membranes may arise from the coexistence of fluid phases or phase-like domains and that critical membrane proteins vary in their intrinsic affinity for these two membrane environments.

To date, only membranes that include cholesterol or other sterols are observed to form Lo membranes (21, 22). Some three-component mixtures that include cholesterol can form continuous membranes that have coexisting domains of Lo and Ld on a size scale that is resolvable by light microscopy (23, 24). The present study makes use of model membranes formed by using several well defined ratios of cholesterol, sphingomyelin (Sph), and dioleoylphosphatidylcholine (DOPC) and other components. Mixtures of these lipids have been used as simple models of the plasma membrane outer leaflet, and the equimolar mixture of cholesterol, Sph, and DOPC has been referred to as a "raft mixture" (25).

Current models describing biological membranes do not directly predict a mechanism by which protein clustering or crosslinking could affect the formation or distribution of different lipid phases. It has been proposed that crosslinking could change the way that a molecule partitions into or out of preexisting domains in the plasma membrane or could coalesce lipid rafts from smaller and/or highly dynamic precursors (1, 2, 26, 27). Our results provide direct evidence that, in model membranes, crosslinking can go beyond the coalescence of preexisting structures and cause uniform one-phase membranes to separate into macroscopic coexisting Lo and Ld phases and that such phase separations can cause a large-scale redistribution of a transmembrane peptide.

Materials and Methods

GM_1, DOPC, dioleoylphosphatidylglycerol, porcine brain Sph, and synthetic stearoyl Sph were purchased from Avanti Polar Lipids. Cholesterol was purchased from Nu Chek Prep (Elysian, MN). Cholera toxin subunit B (CTB) and polyclonal anti-GM_1

This paper was submitted directly (Track II) to the PNAS office.

Abbreviations: Lo, liquid ordered; Ld, liquid disordered; Tmt, miscibility transition temperature; GUV, giant unilamellar vesicle; CTB, cholera toxin subunit B; LAT, linker for activation of T cells; Sph, sphingomyelin; DOPC, dioleoylphosphatidylcholine; DiI, 1,1′-didodecyl-3,3,3′,3′-tetramethylindocarbocyanine.

§To whom correspondence should be addressed at: Department of Molecular Biology and Genetics, Cornell University, 201 Biotechnology Building, Ithaca, NY 14853. E-mail: gwf3@cornell.edu.

www.pnas.org/cgi/doi/10.1073/pnas.0405654102

Table 1. Specific membrane compositions (given as percentage of total by mol)

Text reference	DOPC	DOPG	Sph	Cholesterol	GM_1	Probes	Phase state
Composition a	44.1	4.9	19.0	30.0	2	C12-DiI, perylene	One-phase Ld*
Composition a[1]	44.1	4.9	20.0	30.0	1	C12-DiI, perylene	One-phase Ld*
Composition a[2]	44.1	4.9	20.8	30.0	0.2	C12-DiI, perylene	One-phase Ld*
Composition P	44.1	4.9	19.0	30.0	2	LAT peptide, perylene	One-phase Ld*
Composition b	9.0	1.0	53.0	35.0	2	C12-DiI, perylene	One-phase Lo*
Composition c	45.0	5.0	25.0	23.0	2	C12-DiI, perylene	Two-phase Ld + Lo†
Composition d	43.2	4.8	10.0	40.0	2	C12-DiI, perylene	One-phase unknown
Anchor stock 1	54.4	6.1	0.0	37.5	2	Fast DiI, perylene	One-phase Ld†
Anchor stock 2	32.5	3.8	36.3	23.4	2	Fast DiI, perylene	Two-phase Ld + Lo†
Experimental phase boundary	42.4	4.7	21.8	29.1	2	Fast DiI, perylene	Ld + Lo boundary†

DOPG, dioleoylphosphatidylglycerol.
*Unpublished data.
†This study.

antibody were purchased from Calbiochem. Perylene was purchased from Sigma. C12:0–1,1′-didodecyl-3,3,3′,3′-tetramethylindocarbocyanine (DiI), fast-DiI (C18:2-DiI), and recombinant CTB conjugated with Alexa Fluor 488 (A488-CTB) were obtained from Molecular Probes. The phospholipid stocks were quantitated by phosphate assay, fluorescent dye stocks were quantitated by absorption spectroscopy, and cholesterol and GM_1 stocks were prepared analytically.

Giant Unilamellar Vesicle (GUV) Preparation. GUVs were prepared as described in refs. 28 and 29, with minor modifications. Briefly, lipid mixtures were thoroughly dried from organic solvent into a thin film and hydrated at 65°C by introducing wet N_2 gas. Prewarmed buffer (2.0 mM Mes/10 mM KCl/1.0 mM EDTA, pH 5.5) was added, and the films were incubated overnight to produce GUVs. The suspension was then cooled slowly over 8–16 h to room temperature (23°C). Control samples were tested for possible supercooling by cooling until separation was observed and then rewarming. The prepared GUVs were applied to a standard microscope slide and enclosed by a thin bead of vacuum grease. The sample was sealed with a coverslip, inverted, and imaged on an LCS SP2 confocal microscope (Leica, Deerfield, IL) with a 63× oil-immersion objective at room temperature (23°C). A488-CTB or the anti-GM_1 antibody was added directly to the GUV suspension on the slides and examined immediately. The final concentration of A488-CTB was ≈25 μg/ml, an excess (at least 5-fold) of CTB over GM_1.

The DOPC lipid stock contained 10 mol percent dioleoylphosphatidylglycerol as a charged phospholipid, which is necessary to obtain GUVs by this method. Both stearoyl Sph and brain Sph were used in separate experiments and gave consistent results. The images shown here are with stearoyl Sph. Fluorescent probes were added to the lipid mixture at a molar ratio (probe:total lipid) of 1:1,000 (C12:0-DiI) and 1:250 (perylene). Rhodamine-labeled peptides dissolved in methanol were readily incorporated into GUVs with no alteration of the protocol by mixing the peptide and lipids in organic solvent before preparing the lipid film. Perylene was included in all of the examined GUVs to visualize the Lo phase (30). In every phase-separated membrane, the perylene and C12:0-DiI markers partitioned into opposite phases, and, in the presence of A488-CTB, the perylene and Alexa Fluor 488 patterns overlapped precisely.

GUV preparations yield a highly heterogeneous population of membrane structures that are uniquely suitable for microscopic examination but are not appropriate for bulk measurements such as the fluorescent measurements below. Therefore, a different method was used to prepare the membranes for the fluorescence measurements. Importantly, the phase behavior of membranes prepared by these two methods is consistent (29).

Fluorescence Ratio Method for Phase Boundary Determination. Changes in the fluorescence of differently partitioning probes was monitored as a function of lipid composition (29). Two lipid compositions were chosen to be the endpoint "anchors" of a series of lipid samples. Anchor-stock mixtures of both compositions, including the fluorescent probes fast-DiI and perylene, were prepared in glass vials. These mixtures were placed under high vacuum to remove all solvent and then dissolved in chloroform to 10.0 mM. New anchor stocks were prepared for each independent experiment. Fifty-one defined lipid mixtures were prepared in glass tubes by incrementally mixing the two anchor stocks. Each sample contained 250 nmol of lipid, with the sample compositions evenly spaced in a series between the anchor stocks. Vesicles were prepared from the series of samples by the method of rapid solvent exchange (RSE) (31) to an aqueous buffer (200 mM KCl/5 mM Pipes/1 mM EDTA, pH 7.0). The aqueous lipid concentration of the samples after RSE was 500 μM. Each sample was sealed under argon and placed in a water bath at 65°C. The samples were incubated at 65°C for 2 h, cooled by 2°C/h to 23°C, and held at this temperature for ≈48 h before measurement. Fluorescence was measured at 23°C with a Hitachi 3010 spectrofluorimeter (Hitachi, Tokyo), exciting at 420 nm with a 5-nm bandpass. Perylene emission was measured at 470 nm, and fast-DiI emission was measured at 568 nm with a 10-nm emission bandpass. Each sample was diluted with buffer in the cuvette to a final lipid concentration of 3.75 μM.

For the experiments presented in Fig. 3, the anchor mixtures differed the most in the mol percent of Sph: Anchor stock 1 contained no Sph, whereas anchor stock 2 was more than one-third Sph (Table 1). Anchor stock 2 is a lipid mixture that reproducibly forms Ld plus Lo membranes and is not close to a phase boundary either in composition or temperature (unpublished data; refs. 25 and 32). Anchor stock 1 has the same ratio of DOPC to cholesterol as anchor stock 2 and creates uniform one-phase membranes. Thus, the series of lipid compositions created by this anchor-stock method can be thought of as a titration of Sph that necessarily crosses a phase boundary. Both anchor stocks (and thus the entire series) contained identical amounts of GM_1 and the lipid probes (Table 1). Brain Sph was used in these fluorescence ratio experiments.

Data Fitting. Fluorescence ratio data from the series of lipid compositions were analyzed to determine the intersection of two fluorescence ratio regimes. Two linear regimes were derived from the fluorescence vs. [Sph] data as follows. Any point (x, y) within the data range is chosen to represent the intersection of the regimes. Two unlimited values are chosen; one represents the slope of the regime to the right of the specified point, and the other represents the slope of the regime to the left. With these

four parameters specified, the sum of squares between the fit and the data are assigned as a measure of goodness of fit. The fluorescence vs. [Sph] data space is subdivided at the resolution of the data. Within each subdivision, the four parameters previously described are optimized to yield best-fit values. The four parameters that derive the lowest overall fit value are taken as the global best fit. The lipid composition represented by [Sph] that is associated with the point at the intersection of the two linear regimes is taken as the boundary of the two-phase region. The last six compositions were not used for this analysis because these points clearly do not fit in a linear regime. This choice improves the fit values but has no significant effect on the results. Three independent data sets were fit individually, and the results were averaged.

Miscibility Transition Temperature (Tmt) Measurements. Samples were prepared with or without A488-CTB as for confocal imaging. GUVs were observed by standard fluorescence microscopy by using a 60× water immersion objective on a modified stage that allowed accurate temperature control of a submerged sample. Beginning at a temperature below the Tmt, a GUV was selected, and the sample was warmed at ≈1°C/min. When the observed phases mixed, the temperature detected by a submerged thermocouple was noted. The sample was then set to cool at ≈1°C/min until the vesicle phase separated, and the temperature was noted again.

The temperature measurements were made only on individual vesicles that could be followed through four phase changes without the vesicles touching a glass surface. We designated the average of the four individual measurements (two warming and two cooling) as the Tmt of each observed vesicle. The same procedure was used for samples with A488-CTB added. We find that CTB addition causes the vesicles to become less stable. As a result, the majority of vesicles could not be followed through four phase changes. The incomplete measurements (fewer than four changes), although not used to calculate the Tmt, were uniformly consistent with the final result. Fig. 4 shows the average of four vesicle measurements for each condition.

Linker for Activation of T Cells (LAT). LAT is a plasma membrane protein composed of an intracellular domain, a single membrane-spanning domain, and a 3-aa N-terminal extracellular segment. LAT is doubly palmitoylated near the transmembrane domain. Acylated or not, an N-terminal transmembrane peptide partitions into the Ld phase of two-phase model membranes (33). The unpalmitoylated peptide was incorporated into GUVs at a molar ratio of 1 peptide:500 lipid molecules in the experiments represented in Fig. 2.

Results and Discussion

GUVs. To investigate the effect of crosslinking membrane components, we prepared and examined by fluorescence microscopy GUVs that contain the ganglioside GM_1, which is the natural plasma membrane receptor for cholera toxin (34). Cholera toxin contains five nontoxic B subunits that serve to target the A subunit to cellular plasma membranes. Each CTB pentamer binds specifically to five GM_1 ganglioside molecules. Interestingly, in some cell types, CTB crosslinking of GM_1 initiates signaling cascades (8).

We first examined the partitioning of A488–CTB–GM_1 complexes in membranes that have two coexistent phases, Lo and Ld. These membranes were composed of a mixture of the lipids Sph, cholesterol, and DOPC and included 2 mol percent GM_1 (composition c in Table 1). This mixture of lipids was chosen as a highly simplified model of the outer leaflet of cellular plasma membranes, and, unlike the plasma membrane, the lipids in GUVs of this type are symmetrically distributed between the leaflets. The membranes also included the fluorescent lipid analogs perylene (30) and C12:0-DiI, which preferentially label Lo and Ld phases, respectively. When A488-CTB was added to the GUV samples, A488–CTB–GM_1 complexes were observed to partition strongly into the Lo domain along with the perylene (not shown). This finding has been shown previously in similar lipid mixtures (35, 36) and is consistent with studies of biological membranes, in which gangliosides are well established markers of the raft environment (37, 38).

To analyze the effect of CTB binding and GM_1 crosslinking on the phases of the membrane, GUVs were prepared with molar ratios of the lipid components such that the membranes produced only one uniform phase, either Ld or Lo (compositions a and b, respectively). The fluorescent probes are uniformly distributed in these membranes (Fig. 1 *A* and *E*). Remarkably, the binding of A488-CTB causes the creation of new membrane domains. The initially single-phase membranes now display two coexistent fluid phases, and this change occurs whether the membrane is initially Ld (Fig. 1 *B–D*) or Lo (Fig. 1 *F–H*). The observed changes require the inclusion of GM_1 in the membranes (data not shown). The coexistent domains exhibit rapidly fluctuating boundaries when observed by light microscopy (data not shown), consistent with both phases being fluid (35, 39). Note that the relative amount of the coexisting phases depends on the initial composition (compare Fig. 1 *D* and *H*).

As a control for the possibility that CTB-induced domains are formed by the aggregation of A488-CTB independent of the lipids in the membrane, we examined a lipid mixture that is distinct from the compositions that produce two phases (composition d in Table 1). Although these vesicles looked similar to those of compositions a and b before A488-CTB addition (Figs. 1 *A* and *E* and 2*A*), A488-CTB binding does not cause the formation of resolvable domains in composition d (data not shown). This result indicates that the change in membrane appearance depends on the lipid composition and agrees with previous evidence that CTB does not self-aggregate on membranes (40).

To investigate the effect of this CTB-induced phase change on transmembrane proteins, we prepared experimental membranes (composition P in Table 1) as for Fig. 1 except that the GUVs did not contain C12:0-DiI and included the N terminus of the LAT (see *Materials and Methods*) labeled with rhodamine (33). This peptide includes the single transmembrane domain of the LAT protein, which is critically involved in T cell receptor and FcεRI signaling (41, 42). A488-CTB binding and the resultant membrane reorganization cause the LAT transmembrane domain to concentrate in the new Ld phase (Fig. 2), consistent with previous observations of the partitioning behavior of this polypeptide in a variety of phase-separated model membranes (33). Thus, the changes in phase behavior caused by A488-CTB binding alter the distribution of the transmembrane region of this functionally important plasma membrane protein.

We expect that GM_1 and CTB must have minimum effective concentrations for the observation of the CTB-induced phase changes. Large phase separations were readily observed in membranes in which the mol percent of GM_1 was reduced by half (composition a^1 in Table 1), whereas at 0.2 mol percent GM_1 (composition a^2), fewer than half of the GUVs examined were phase-separated after A488-CTB addition. We also varied the concentration of A488-CTB during the slide preparations. At 1/10 the final A488-CTB concentration (≈3 μg/ml) composition a vesicles were slightly less bright, but this concentration was fully capable of inducing phase changes (data not shown). Concentration limits are likely to be highly dependent on the specific lipid composition and the properties of the crosslinked molecule. Therefore, such limits will not be predictive for biological systems where crosslinking is implicated.

CTB is a pentamer and is probably crosslinking five GM_1 gangliosides in these experiments. We were unable to observe a

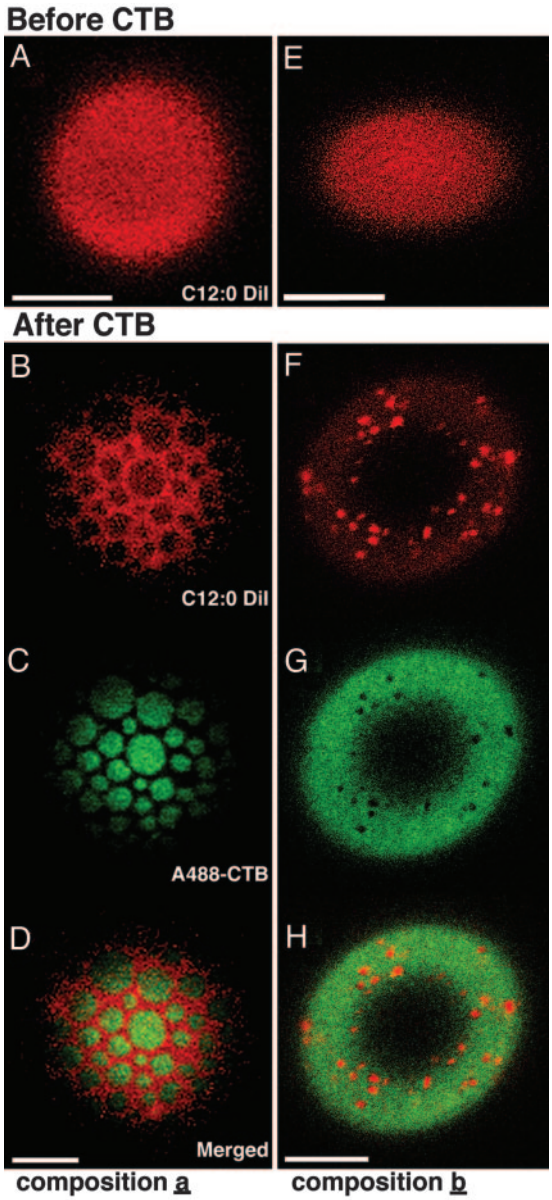

Fig. 1. CTB binding changes the phase behavior of membranes containing the ganglioside GM_1. GUVs labeled with C12:0-DiI were examined before and after the addition of A488-CTB by imaging grazing focal planes by confocal microscopy. (*A* and *E*) C12:0-DiI in single-phase vesicles [composition a (*A*) and b (*E*) in Table 1] before the addition of A488-CTB. (*B–H*) Upon the addition of A488-CTB, the vesicles undergo a phase transition yielding coexistent fluid phases. A488-CTB decorates the Lo phase (*C* and *G*); C12:0-DiI labels the Ld phase (*B* and *F*). *D* and *H* are the merged images of *B*/*C* and *F*/*G*, respectively. (Scale bars, 5 μm.)

phase change after the binding of an anti-GM_1 antibody to GUVs of composition a (Table 1 and data not shown). A simple explanation is that dimerization is less effective at causing a phase change than crosslinking with higher valency by CTB.

Determining the Phase Boundary. From the microscopy observations, the membranes appear to phase-separate in response to the binding of A488-CTB to the GM_1 incorporated in the membrane. An important alternate possibility is that the membranes are actually phase-separated before A488-CTB is added but that one phase exists in distributed structures below the size resolution of light microscopy. In this interpretation, A488-CTB

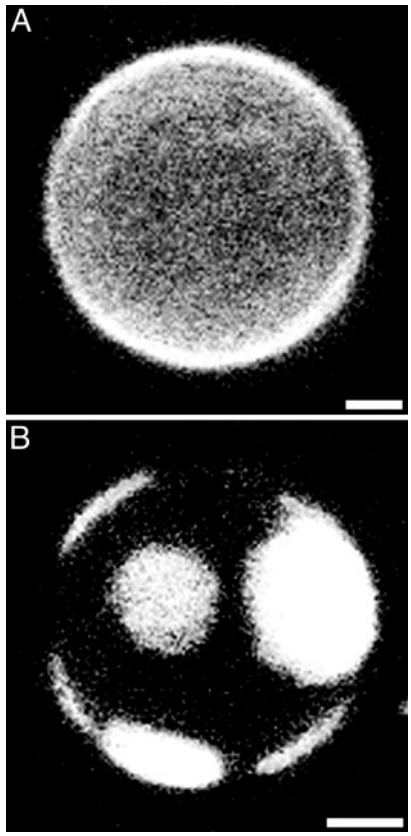

Fig. 2. CTB binding to GM_1 in the membrane indirectly changes the distribution of the transmembrane peptide of LAT by changing the phase state of the lipid bilayer. GUVs of composition P (Table 1), containing rhodamine-labeled LAT peptides (1:500 mol ratio, peptide to lipid), were examined before (*A*) and after (*B*) the addition of A488-CTB. The images are the projection of a stack of confocal slices from one hemisphere of representative GUVs and show the pattern of rhodamine fluorescence (bright areas). The dark areas are Lo phase as determined by the partitioning of perylene (not shown). (Scale bars, 5 μm.)

binding would coalesce the unresolved phase into larger structures. This possibility is interesting in the context of the lipid raft hypothesis, because lipid rafts are apparently too small to resolve in unperturbed living cells (26, 43). However, further analysis below, using methods that are not limited by optical resolution, strongly favors the interpretation that CTB binding to the membranes creates new phases.

To test whether membranes of composition a (Table 1) used in the GUV studies (Figs. 1*A* and 2*A*) are one phase before the addition of CTB, we made use of a fluorescence ratio method for determining the composition of phase boundaries (see *Materials and Methods*). For this determination, the ratio of fluorescence of two lipid analogs (in this case, fast-DiI and perylene) is measured. The excitation of DiI by this method is due to FRET from perylene. The simple ratio of fast-DiI to perylene fluorescence (corrected for background) is not corrected for either dependence of perylene or DiI fluorescence on sample composition or self-quenching of the dye. As a result, the measured fluorescence ratio is sensitive to changes in lipid environment because of several factors: (*i*) the probes separate from each other; hence, FRET decreases when Lo and Ld phases form and separate, (*ii*) even within a one-phase region, DiI fluorescence can vary significantly with membrane composition (unpublished data), and (*iii*) DiI fluorescence depends on the dye concentration within a phase (self-quenching).

We determined the one-phase/two-phase boundary by mea-

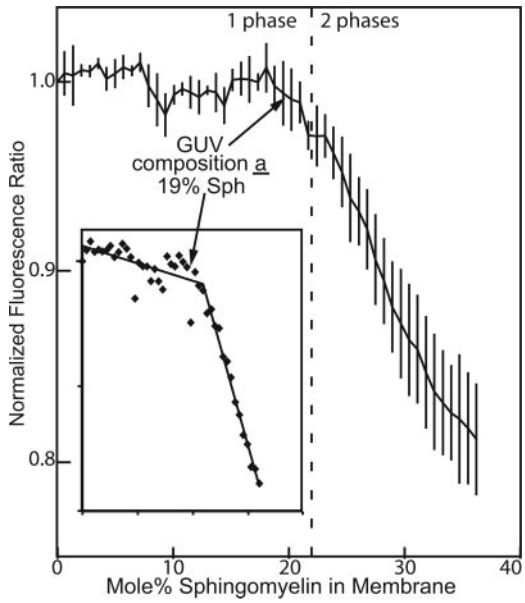

Fig. 3. The membrane composition used in GUV preparations forms single-phase membranes and is close to a phase boundary. A series of membranes that represent a titration of Sph into a mixture of cholesterol and DOPC (with the [DOPC]:[cholesterol] held constant) was analyzed by a fluorescence ratio method (see *Materials and Methods*). The graph shows the average of measurements from three independent experiments. Each data set was normalized to one for the initial values and then averaged. The vertical bars indicate the standard deviation. The *x* axis is the amount of Sph in the membranes, presented as the percent by mol of total membrane components. The vertical dashed line indicates the average experimental phase boundary, 22 mol percent Sph, as determined by our fitting analysis (see *Materials and Methods*). Composition a (Table 1), corresponding to GUV images (Figs. 1*A* and 2*A*), is indicated with arrows. (*Inset*) The normalized data from one individual experiment plotted on the same axes as the larger graph (diamonds). The solid line represents the calculated best fit of two linear regimes that intersect at the phase boundary.

suring an experimental series of 51 membrane compositions that includes composition a (Fig. 3). This series of membranes is an incremental titration of Sph that crosses the phase boundary that we wish to define. The amount of incorporated GM_1 and fluorescent dyes remained constant throughout the series. Fig. 3 shows how the fluorescence ratio changes as the percentage of Sph is increased. The observed changes are readily divided into two regimes that correspond to an almost horizontal, single-phase regime at low Sph percentages and a negatively sloped, two-phase regime at higher Sph percentages. The point at which the slope changes is the phase boundary. Membranes of composition a (Table 1) are within the one-phase regime and close to the boundary (Fig. 3), consistent with the images of the corresponding GUVs (Figs. 1*A* and 2).

By fitting the fluorescence data to two lines that intersect (see *Materials and Methods*), it is possible to quantitate the experimental phase boundary. The fit analysis yields a boundary of 21.8 ± 0.35 mol percent Sph. The experimental data supports two significant figures in this measurement, or 22 mol percent Sph (3 mol percent higher than composition a). Therefore, we conclude that in GUVs with the same composition, the A488–CTB–GM_1 binding-dependent domains that we observe by microscopy are not formed by the coalescence of preexisting phases.

Measuring CTB-Induced Changes in Phase Boundaries. We also attempted to determine the phase boundary in membranes in the presence of bound CTB by using several versions of the fluorescence ratio method (see *Materials and Methods*). CTB addition caused the experimental boundary to change in the expected direction (i.e., to a lower mol percent Sph) in every experiment, with an average shift of −3.3 ± 3.3 mol percent Sph (five independent experiments). However, we note that the standard deviation of these measurements is 10-fold higher than the measurements without CTB. A primary limitation in assessing the effects of CTB on the fluorescence ratio is that the rapid solvent exchange method creates mixtures of unilamellar and multilamellar vesicles, such that an average of 1.4 lamellae are produced with our apparatus (31). Because only the outermost membrane of a multilamellar vesicle is accessible to CTB, a fraction of the membrane in each sample will not undergo the CTB-induced phase changes. Furthermore, the vesicles vary in size (down to <100 nm), and it is not determined what effect curvature has on CTB binding or the observed change in phase behavior. We believe that these considerations could explain the increased sample-to-sample variation that we see only after CTB addition. Further refinement of the method will be required to accurately measure the CTB-induced change at this phase boundary.

To determine more accurately whether CTB binding can cause a significant change in a phase boundary, we measured the Tmt of model membranes before and after A488-CTB was added to bind to incorporated GM_1. Membranes with coexistent fluid phases have a characteristic Tmt, at which the membrane reversibly converts between having two phases and only one phase. We measured the Tmt of GUVs that have both Lo and Ld phases at 23°C (composition c in Table 1) before and after the

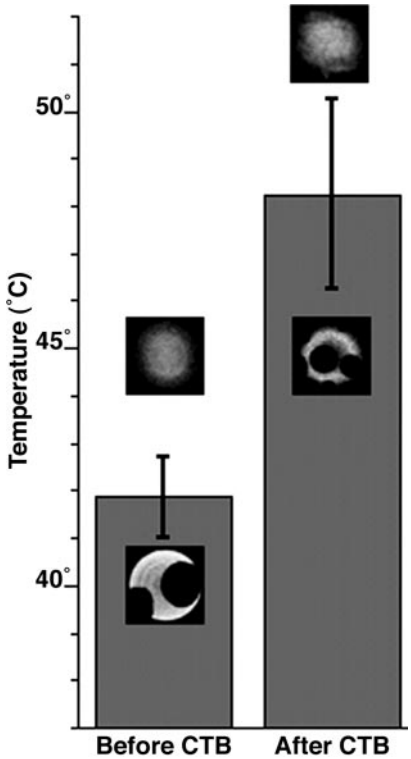

Fig. 4. CTB binding causes an increase in the Tmt. The Tmt of membranes of composition c (Table 1) was measured before and after introduction of A488-CTB. Individual GUVs were observed through at least two cycles of slow heating until the phases mixed, followed by slow cooling until the phase separated again. The graph shows the average values from four such measurements, and the error bars show the standard deviation. (*Insets*) Examples of C12:0-DiI-labeled GUVs illustrating the conversion from one phase to two phases at the Tmt.

introduction of A488-CTB (Fig. 4). The measurements are performed on a microscope by observing individual GUVs as the sample temperature is gradually cycled up and down across the transition point.

We observe an ≈6°C average increase in the Tmt of these GM_1-containing vesicles after A488-CTB binding (Fig. 4). The measured CTB-induced shift in the Tmt was confirmed by other observations of the membranes. For example, a sample without CTB was slowly raised to 44°C and allowed to equilibrate for 10 min. No membranes were found that showed phase separation. Then, A488-CTB was added to a sample from the same vesicle preparation and equilibrated at 45°C for 10 min. The GUVs in this sample showed clear phase separation. This shift in the Tmt of the membranes indicates that A488-CTB binding to GM_1 can cause a measurable shift in a phase boundary.

Implications. We conclude that in lipid bilayers, CTB binding to its receptor (GM_1) can cause the membrane to phase-separate, and we demonstrate that such a phase separation can directly alter the distribution of a peptide derived from a membrane protein. Apparently, this change in membrane phase behavior is caused by crosslinking GM_1 molecules due to the pentameric binding of CTB to GM_1, although we cannot exclude the contributions, if any, of interactions between the membrane-proximal surface of GM_1-bound CTB and other lipid head groups.

The lipid composition of a membrane is crucial for observing large-scale CTB-induced phase changes. However, we predict that the physical properties of any GM_1-containing membrane, regardless of composition, will be altered by the binding of CTB. Such changes would likely result in modest differences in the chemical potential and mixing properties of specific molecules and would be most readily detected by changes in the relative surface fraction of two coexistent phases and changes in the partitioning coefficient of probe molecules. In support of this prediction, we note two minor observations made during the course of these studies. First, the fluorescence ratio measurements shown in Fig. 3 are altered by the binding of CTB, regardless of the composition of the membrane (not shown). Second, in Fig. 1 *A–D*, CTB binding causes the vesicle to have islands of Lo phase in a continuous Ld membrane, whereas in Fig. 2, a similar lipid composition (with a peptide added) forms continuous Lo phase with islands of Ld in response to CTB. It will be informative to examine the physical effects of crosslinking other components in both model and cellular membranes.

Our results provide one possible explanation for how a cell detects an extracellular crosslinking event or organizes a domain in response to the local clustering of specific components: Crosslinking a membrane component could significantly alter the mixing properties of the lipid bilayer and dramatically alter the localization of important proteins and lipids. Such mechanisms have been suggested as potential models of lipid raft behavior in cells (1, 2, 26, 27). The initial reorganization could be cumulatively stabilized by a subsequent cascade of protein–protein interactions. In this way, the organization of the underlying membrane could be used as a device by which changes in the distribution of one membrane protein affect the distribution of many other proteins. In cellular processes, such crosslinking effects would almost certainly be initialization events, local and heterogeneous, rather than encompassing the entire cell, consistent with the dynamic nonequilibrium properties of complex cellular membranes.

We thank Andrew Smith for unpublished experimental data defining a phase diagram that informed our choice of lipid compositions; Jeff Buboltz for the anchor-stock method and for originally developing the fluorescence ratio method; David Stringer for his work on the fluorescence ratio method; the Microscopy, Imaging, and Fluorimetry Facility at Cornell University and Carol Bayles for expert technical assistance; Hidehiko Shogomori, Deborah Brown, and Erwin London (all of State University of New York, Stony Brook) for the synthesized LAT peptide and critical reading of the manuscript; Michael Edidin for critical editing and discussions; and Andrew Rice and Watt Webb for productive discussions. This work was supported by grants from the Keck Foundation, the Resource for Biophysical Imaging Opto-Electronics, the National Center for Research Resources (P41-RR04224), the National Institutes of Health (AI18306 and GM08267), and the National Science Foundation (MCB-0315330).

1. Brown, D. A. & London, E. (1998) *J. Membr. Biol.* **164,** 103–114.
2. Edidin, M. (2003) *Annu. Rev. Biophys. Biomol. Struct.* **32,** 257–283.
3. Dustin, M. L. (2002) *Cell* **110,** 13–18.
4. Chazal, N. & Gerlier, D. (2003) *Microbiol. Mol. Biol. Rev.* **67,** 226–237.
5. Bagnat, M. & Simons, K. (2002) *Biol. Chem.* **383,** 1475–1480.
6. Anderson, R. G. & Jacobson, K. (2002) *Science* **296,** 1821–1825.
7. Holowka, D. & Baird, B. (2001) *Semin. Immunol.* **13,** 99–105.
8. Janes, P. W., Ley, S. C. & Magee, A. I. (1999) *J. Cell Biol.* **147,** 447–461.
9. Grakoui, A., Bromley, S. K., Sumen, C., Davis, M. M., Shaw, A. S., Allen, P. M. & Dustin, M. L. (1999) *Science* **285,** 221–227.
10. Dykstra, M., Cherukuri, A., Sohn, H. W., Tzeng, S. J. & Pierce, S. K. (2003) *Annu. Rev. Immunol.* **21,** 457–481.
11. Simons, K. & Ikonen, E. (1997) *Nature* **387,** 569–572.
12. Pierini, L. M. & Maxfield, F. R. (2001) *Proc. Natl. Acad. Sci. USA* **98,** 9471–9473.
13. Parton, R. G. & Richards, A. A. (2003) *Traffic* **4,** 724–738.
14. Slimane, T. A., Trugnan, G., Van, I. S. C. & Hoekstra, D. (2003) *Mol. Biol. Cell* **14,** 611–624.
15. Field, K. A., Holowka, D. & Baird, B. (1997) *J. Biol. Chem.* **272,** 4276–4280.
16. Pierini, L. M., Eddy, R. J., Fuortes, M., Seveau, S., Casulo, C. & Maxfield, F. R. (2003) *J. Biol. Chem.* **278,** 10831–10841.
17. Luzzati, V. & Husson, F. (1962) *J. Cell Biol.* **12,** 207–219.
18. Dodge, J. T. & Phillips, G. B. (1967) *J. Lipid Res.* **8,** 667–675.
19. Singer, S. J. & Nicolson, G. L. (1972) *Science* **175,** 720–731.
20. Edidin, M. (2003) *Nat. Rev. Mol. Cell. Biol.* **4,** 414–418.
21. Shimshick, E. J. & McConnell, H. M. (1973) *Biochem. Biophys. Res. Commun.* **53,** 446–451.
22. Ahmed, S. N., Brown, D. A. & London, E. (1997) *Biochemistry* **36,** 10944–10953.
23. Veatch, S. L. & Keller, S. L. (2003) *Biophys. J.* **85,** 3074–3083.
24. Dietrich, C., Volovyk, Z. N., Levi, M., Thompson, N. L. & Jacobson, K. (2001) *Proc. Natl. Acad. Sci. USA* **98,** 10642–10647.
25. Veatch, S. L. & Keller, S. L. (2003) *Biophys. J.* **84,** 725–726.
26. Kusumi, A., Ike, H., Nakada, C., Murase, K. & Fujiwara, T. (2005) *Semin. Immunol.* **17,** 3–21.
27. Simons, K. & Toomre, D. (2000) *Nat. Rev. Mol. Cell Biol.* **1,** 31–39.
28. Akashi, K., Miyata, H., Itoh, H. & Kinosita, K., Jr. (1996) *Biophys. J.* **71,** 3242–3250.
29. Feigenson, G. W. & Buboltz, J. T. (2001) *Biophys. J.* **80,** 2775–2788.
30. Baumgart, T., Hess, S. T. & Webb, W. W. (2003) *Nature* **425,** 821–824.
31. Buboltz, J. T. & Feigenson, G. W. (1999) *Biochim. Biophys. Acta* **1417,** 232–245.
32. Stottrup, B. L., Stevens, D. S. & Keller, S. L. (2005) *Biophys. J.* **88,** 269–276.
33. Shogomori, H., Hammond, A. T., Barr, D. J., Feigenson, G. W., London, E. & Brown, D. A. (2005) *J. Biol. Chem., in press.*
34. Lencer, W. I., Hirst, T. R. & Holmes, R. K. (1999) *Biochim. Biophys. Acta* **1450,** 177–190.
35. Dietrich, C., Bagatolli, L. A., Volovyk, Z. N., Thompson, N. L., Levi, M., Jacobson, K. & Gratton, E. (2001) *Biophys. J.* **80,** 1417–1428.
36. Kahya, N., Scherfeld, D., Bacia, K., Poolman, B. & Schwille, P. (2003) *J. Biol. Chem.* **278,** 28109–28115.
37. Brown, D. A. & Rose, J. K. (1992) *Cell* **68,** 533–544.
38. Parton, R. G. (1994) *J. Histochem. Cytochem.* **42,** 155–166.
39. Seul, M. & Andelman, D. (1995) *Science* **267,** 476–483.
40. Cai, X. E. & Yang, J. (2003) *Biochemistry* **42,** 4028–4034.
41. Saitoh, S., Arudchandran, R., Manetz, T. S., Zhang, W., Sommers, C. L., Love, P. E., Rivera, J. & Samelson, L. E. (2000) *Immunity* **12,** 525–535.
42. Zhang, W., Sloan-Lancaster, J., Kitchen, J., Trible, R. P. & Samelson, L. E. (1998) *Cell* **92,** 83–92.
43. Munro, S. (2003) *Cell* **115,** 377–388.